Single Carbon Nanotube Optical Spectroscopy

Achim Hartschuh,[b, c] Hermenegildo N. Pedrosa,[a] Jeffrey Peterson,[a] Libai Huang,[a] Pascal Anger,[b] Huihong Qian,[b] Alfred J. Meixner,[b] Mathias Steiner,[b] Lukas Novotny,[c] and Todd D. Krauss*[a]

This Minireview discusses novel insights into the electronic structure of carbon nanotubes obtained using single-molecule fluorescence spectroscopy. Fluorescence spectra from single nanotubes are well described by a single, Lorentzian lineshape. Nanotubes with identical structures fluoresce with different energies due to local electronic perturbations. Carbon nanotube fluorescence unexpectedly does not show any intensity or spectral fluctuations at 300 K. The lack of intensity blinking or bleaching demonstrates that carbon nanotubes have the potential to provide a stable, single-molecule infrared photon source, allowing for the exciting possibility of applications in quantum optics and biophotonics.

1. Carbon Nanotube Optical Properties

Single-walled carbon nanotubes (SWNTs) are tubular graphitic molecules that can be microns long and less than one nanometer wide. The combination of the unique properties of the carbon–carbon bond and their interesting molecular structure have given SWNTs unique physical properties and provided the potential for revolutionary applications.[1–4] SWNT structure is characterized by two integers (*n*,*m*) that can be easily related to both its diameter and chirality.[1] SWNTs have an unusual electronic configuration: each SWNT with a distinct (*n*,*m*), where *n*–*m* divisible by three is metallic, while the rest are semiconducting.[5,6] Further, SWNT electronic properties exhibit a strong structural dependence,[1] which helps drive potential applications.

Simple one-electron models indicate that the density of states (DOS) of a nanotube is characterized by singularities, with each singularity corresponding to a quantum subband (Figure 1).[7] Recent studies of individual SWNT electronic structure using scanning tunneling spectroscopy (STS)[5,6,8] agree with these general predictions. Simple one-electron models also imply that the dipole-allowed optical transitions occur between mirror image peaks in the DOS (Figure 1). Absorption spectra of SWNT bundles contain three broad absorption regions corresponding to the first and second allowed transitions for semiconductor SWNTs, and the first allowed transition for metallic SWNTs, respectively (Figure 2). However, these spectra do not exhibit any features identified with a particular nanotube structure, since strong electronic coupling mixes the energy states from the different SWNTs in the bundle.[9] This strong intertube coupling, combined with the large inhomogeneity in nanotube structures present in an ensemble, completely obscures any fine structure in the absorption spectra.

Isolation of individual nanotubes is critical for decoupling the optical response of one nanotube from another, and was recently demonstrated by O'Connell et al. for nanotubes manufactured by the high-pressure CO chemical vapor deposition (HiPCo) process (H-SWNTs).[10] As shown in Figure 3 A, absorption spectra of an ensemble of isolated SWNTs (Mic-SWNTs) show many more highly resolved features than the corresponding absorption spectrum from nanotube bundles. These distinct features correspond to dipole-allowed optical transitions from SWNTs with different (*n*,*m*) values[11] and/or from higher interband transitions for a nanotube with a given (*n*,*m*) value. The general isolation procedure can be applied using numerous surfactants,[12] as well as nanotubes produced by various methods such as the laser oven (L-SWNTs), and arc discharge (A-SWNTs) processes (Figure 3 A).

Bundled SWNTs do not fluoresce since any metallic tubes present in the bundle provide an efficient nonradiative pathway for photoexcited electrons. However, as first demonstrated in ref. [10] for HiPCo SWNTs, Mic-SWNT samples show strong, dipole allowed fluorescence at the band-edge (Figure 3 B). The measured Stokes shift between the absorbing and emitting lines is quite small ($\approx 40\ cm^{-1}$).[10] SWNTs are poor emitters; the fluorescence quantum yield (QY) of SWNTs is on the order of QY $\approx 10^{-4}$.[13]

The dependence of the SWNT electronic structure on diameter and chirality [(*n*,*m*) values] is fundamentally important and is also of technical interest. Simple one-electron models predict that the energy of the dipole-allowed optical transitions depends linearly on the nanotube diameter.[14] However, the observation of structurally dependent photoluminescence from SWNTs represented a major breakthrough,[11] as the dependence of electronic transition energies was shown to depend on (*n*,*m*) values explicitly and not simply on the SWNT diameter.[11] In particular, the magnitude and sign of deviations from the

[a] *H. N. Pedrosa, J. Peterson, L. Huang, Prof. T. D. Krauss*
Department of Chemistry, University of Rochester
Rochester, New York 14627 (USA)
Fax: (+1) 585-276-0205
E-mail: krauss@chem.rochester.edu

[b] *Prof. Dr. A. Hartschuh, P. Anger, H. Qian, Prof. Dr. A. J. Meixner, M. Steiner*
Physikalische Chemie I, Universität Siegen
57068 Siegen (Germany)

[c] *Prof. Dr. A. Hartschuh, Prof. L. Novotny*
The Institute of Optics, University of Rochester
Rochester, New York 14627 (USA)

 DOI: 10.1002/cphc.200400408 © 2005 Wiley-VCH Verlag GmbH & Co. KGaA, Weinheim

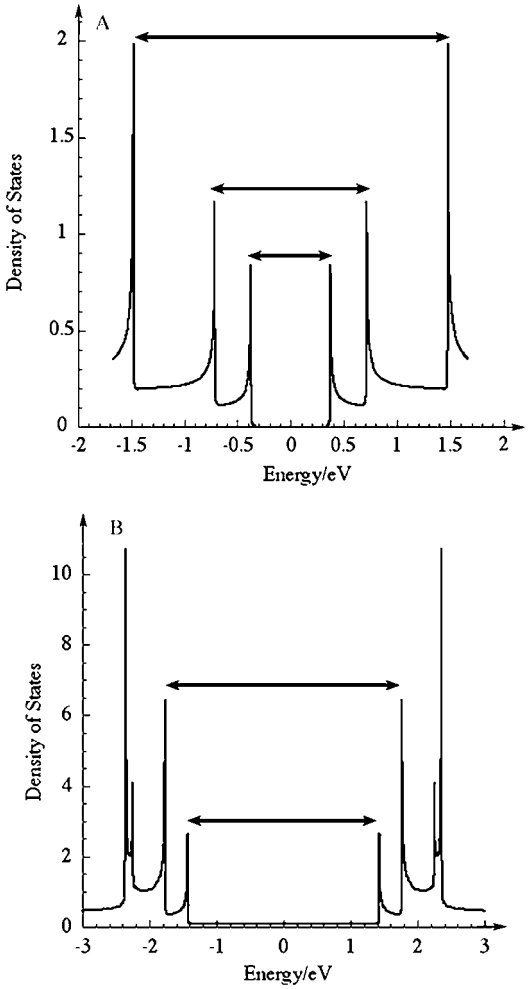

Figure 1. Calculated density of states for A) a (10,5) nanotube and B) a (9,0) nanotube within the tight-binding approximation. The absence of electronic states at the Fermi level (0 eV) indicates the (10,5) tube is semiconducting, while the presence of electronic states at the Fermi level indicates the (9,0) nanotube is metallic. The arrows correspond to dipole-allowed optical transitions.

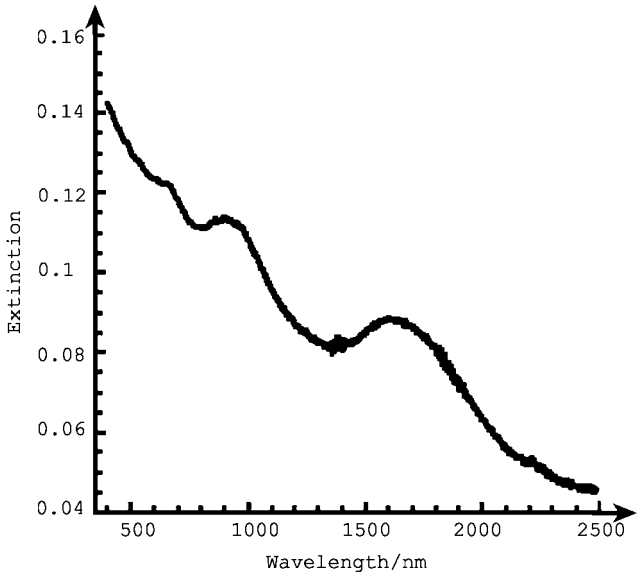

Figure 2. Optical absorption spectrum of SWNTs spun coat from toluene onto quartz. The peaks at 1700 and 950 nm are due to semiconducting nanotubes, and the peak at 650 nm is due to metallic nanotubes. SWNTs were obtained from Tubes@rice and produced by the laser-oven method.

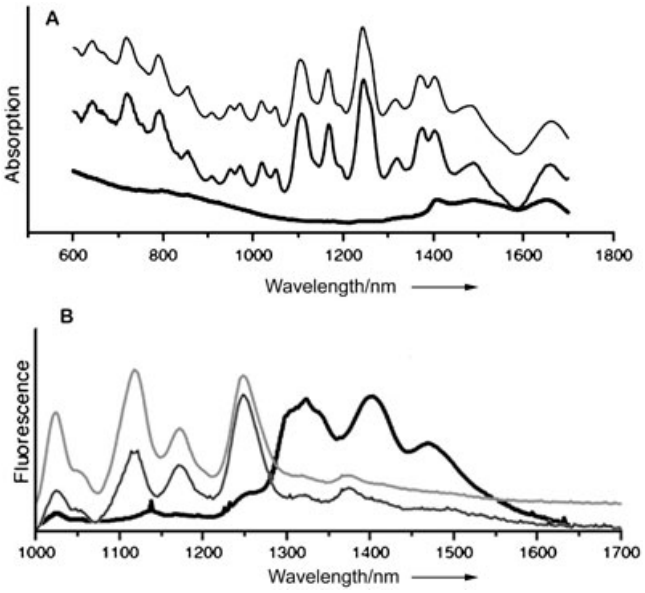

Figure 3. Absorption (A) and fluorescence (B) spectra of Mic-SWNT samples isolated in surfactant micelles in D_2O according to ref. [10]. The top, middle and bottom curves correspond to H-SWNTs, A-SWNTs, and L-SWNTs, respectively. Spectra are vertically offset for clarity. Due to detector responsivity fluorescence spectra do not extend past 1650 nm.

predicted linear dependence were observed to depend on the value of (n-m) mod 3,[11] suggesting that trigonal warping effects[15] were playing a significant role. Empirical fitting parameters have been introduced modifying the simple one-electron picture to compensate for these effects,[11,16] thus allowing for a precise prediction of the transition energies for different tube (n,m) structures. However, despite the observation of fluorescence spectral features attributable to specific nanotube (n,m) structures, it is not fully understood why the transition frequencies differ significantly from simple theoretical predictions,[11] although many-particle interactions[17,18] and/or trigonal warping effects[15] likely play a role in this discrepancy.

Notwithstanding these recent advances in SWNT separation and isolation, the optical spectra shown in Figure 3 clearly suffer from severe inhomogeneous broadening due to the distribution of different nanotube structures in the ensemble. Thus, early optical studies could only determine an averaged overall behavior that obscured crucial electronic characteristics of the individual nanotube.[10,11,19–21] For example, since spectra from SWNTs with different (n,m) values will overlap, it is difficult to make definite conclusions regarding important emission features such as the spectral line width or details of the band shape, or to observe evidence of coupling to vibrations. Therefore, new approaches are needed to further advance the understanding of SWNT optical properties and accelerate the de-

 © 2005 Wiley-VCH Verlag GmbH & Co. KGaA, Weinheim

velopment of novel SWNT photonic applications, such as nanometer scale integrated electroluminescent devices.[22]

2. Single Nanotube Fluorescence

Spin-casting the Mic-SWNT suspension onto a cover slip allows for isolation of individual nanotubes by standard confocal microscopy (Figure 4). A typical fluorescence image from the spun Mic-SWNT sample is shown in Figure 5, with a spatial resolution of 300 nm. The image was obtained by collecting an optical spectrum at every pixel and then binning regions of the individual spectra where strong fluorescence signals are expected according to the ensemble spectrum (Figure 3B). Since atomic force microscopy (AFM) measurements reveal predominantly short SWNTs (length 200–300 nm) lying on top of residual surfactant patches, distinct tubular features in the Mic-SWNT fluorescence images are typically unresolved. Alternatively, by dispersing SWNTs directly in organic solvents such as dichloroethylene, followed by spin coating, occasionally individual nanotubes that fluoresce can be isolated, as shown in Figure 6. In Figure 6 both the fluorescence and Raman images clearly show the characteristic one-dimensional features of the SWNT thus proving that the fluorescence in fact results from the single nanotube.

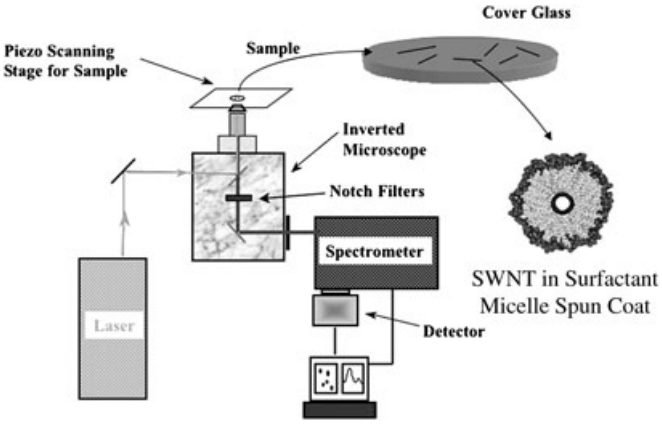

Figure 4. *Standard confocal microscopy setup for observing fluorescence from individual SWNTs. Excitation was typically at 633 nm (tunable dye laser) with intensities on the order of 40 kW cm^{-2}. Laser excitation at 633 nm ensures that all Raman signals between 633 and 770 nm are spectrally distinct from the fluorescence signals above 850 nm.*

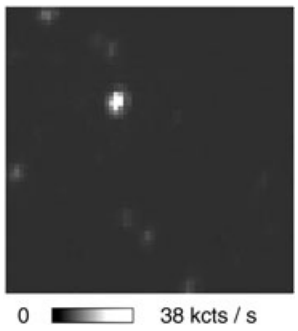

Figure 5. *Typical confocal fluorescence image (10×10 μm^2) of single spatially isolated SWNTs on glass acquired by raster scanning the sample and simultaneous detection of an optical spectrum at every pixel. The image contrast was obtained by integrating the detected spectrum between 945–975 nm.*

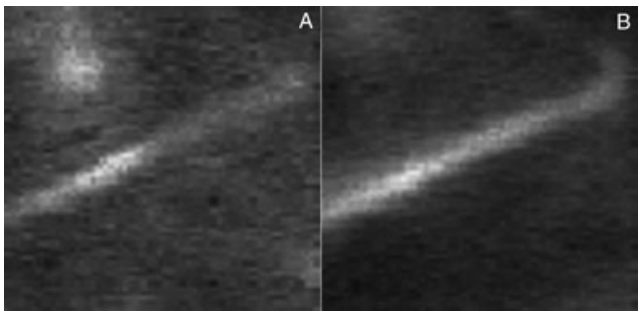

Figure 6. *A) Fluorescence image (2.5×2.5 μm^2) of a single spatially isolated SWNT on glass. The image was obtained by filtering the detected optical emission between 925–975 nm. B) Resonance Raman image from the same area as (A). The image represents a spatially resolved detection of the tangential (G-band) at 1550 cm^{-1}.*

Fluorescence images from the isolated Mic-SWNTs show distinct, bright spots at different positions for different emission wavelengths.[23] Figure 7 displays representative spectra detected from one of these bright spots. Each spectrum now exhibits a single emission band with a smooth line shape; all traces of contributions to the fluorescence spectra from the different SWNT *(n,m)* structures have been eliminated.[23] The fluorescence maximum for all three spectra matches three transitions observed in the ensemble spectrum (Figure 3B). In so much as the ensemble fluorescence spectrum is a weighted superposition of spectra from individual SWNTs, the spectra in Figure 7 are attributed to individual SWNTs.[23]

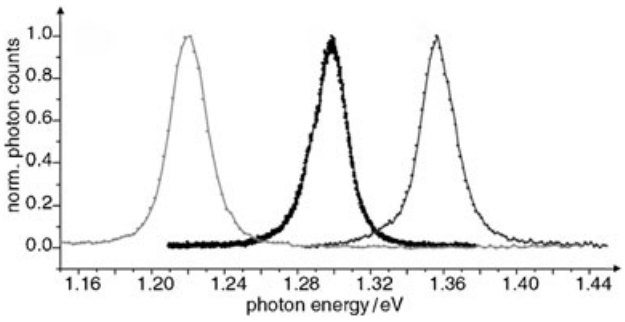

Figure 7. *Fluorescence spectra detected for three different sample positions. Fluorescence maxima are at wavelengths of 1016, 955, and 914 nm, respectively, from left to right.*

Single nanotube spectroscopy clearly eliminates the overlapping spectral features associated with ensemble averaging and thus allows for the potential discovery of crucial SWNT optical and electronic properties. For example, SWNT fluorescence spectra are described by a single, featureless, symmetrical

 © 2005 Wiley-VCH Verlag GmbH & Co. KGaA, Weinheim

band corresponding to a single Lorentzian line shape function (solid lines in Figure 7). The room-temperature-broadened fluorescence line width is approximately 23 meV, in agreement with the approximately 25 meV linewidths reported in ref. [10] for fluorescence from macroscopic samples. Also, single nanotube spectroscopy reveals that the fluorescence spectra from SWNTs with identical (*n*,*m*) structural parameters are not the same. Indeed, as shown in Figure 8 fluorescence spectra from

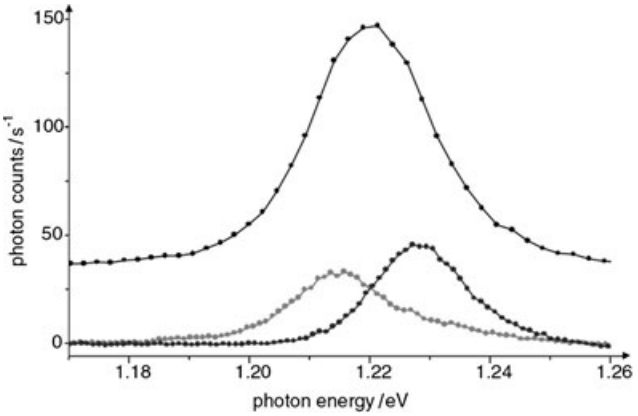

Figure 8. *Fluorescence spectra for three individual (7,5) SWNTs at different positions on the substrate. The spectral position, amplitude, and shape of the emission bands differ substantially. The spectra are offset for clarity.*

SWNTs with the same structure can be significantly different. This deviation suggests that SWNT fluorescence may come from trap states caused by structural[24–26] or chemical defects. Alternatively, the deviations in fluorescence energy could arise from perturbations in the electronic band structure due to fluctuations in the local environment, such as from electrostatic surface potential changes[27] or localized charges.[28] Some insight is provided by recent experiments whereby fluorescence from only (*6*,*4*) SWNTs was monitored. As shown in Figure 9, as the excitation wavelength is tuned, different nanotubes in the optical image move in and out of resonance. Thus, different nanotubes with the same *(n*,*m)* structure have different absorption energies (and therefore different electronic properties) arising from an inhomogeneity in their local environments.

Assignment of a SWNT (*n*,*m*) structure with a particular optical transition relies on correlating that spectral feature with the radial breathing mode (RBM) frequency through resonant Raman scattering. For macroscopic samples this connection is difficult, since uncertainties in parameters used for calculating the relevant (resonant) optical transition energy,[16] and the cluster of different SWNT structures with similar diameters lead to several possibilities for assignments.[11,16] Thus, complicated fitting procedures were employed to assign optical transition energies to particular (*n*,*m*) values.[11,16] Single nanotube spectroscopy has the advantage in that it allows for a direct assignment of fluorescence energies to specific *(n*,*m)* nanotube structures without any ambiguity arising from using complicated fitting procedures (Table 1). Thus, as a result of the single

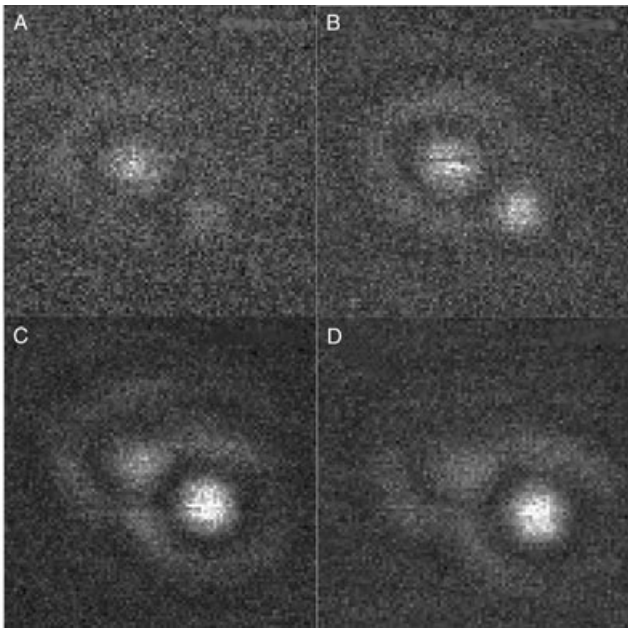

Figure 9. *Fluorescence images acquired through an 880 $\pm$ 20 nm filter that selects fluorescence from only (6,4) nanotubes. The excitation wavelength is A) 600 nm, B) 595 nm, C) 580 nm, D) 575 nm. Scan range is 2.3 $\times$ 2.3 μm.*

Table 1. *Spectral data and structural assignments for SWNTs. λ_{Em} ($h\nu_{Em}$) is the measured average fluorescence wavelength (energy). ν_{RBM} is the SWNT radial breathing mode frequency. The literature values agree with the assignments in ref. [11].*

λ_{Em} [nm]	$h\nu_{Em}$ [eV]	$h\nu_{Em}$ [eV] (literature)	Observed ν_{RBM} [cm^{-1}] $\pm$3 cm^{-1}	Predicted ν_{RBM} [cm^{-1}]	(*n*,*m*) Assignment
1023	1.212	1.212	282	281.9	(7,5)
976	1.270	1.272	308	307.4	(6,5)
955	1.298	1.302	296	298.1	(8,3)
915	1.355	1.359	309	307.4	(9,1)
881	1.407	1.420	337	335.2	(6,4)

nanotube spectroscopic measurements, the assignments as given in ref. [11] were directly confirmed.

3. SWNT Fluorescence Intermittency

The fluorescence from individual semiconductor quantum dots,[29–32] and from small molecules,[33,34] exhibit an emission intermittency or on-off "blinking" behavior for all excitation intensities, all temperatures, and on time-scales spanning many orders of magnitude (Figure 10).[35] In fact, fluorescence intermittency is commonly used as the conclusive indicator of single chromophore optical emission. Surprisingly, the fluorescence intensity from a single SWNT at 300 K recorded using moderate excitation intensities ($<$ 70 kW cm^{-2}) is constant over many seconds with no indication of fluctuations on the 40-ms to 100-second time scale (Figure 10 A).[23] At extremely high excitation powers ($>$ 100 kW cm^{-2}), fluorescence intensity fluctuations can be observed, likely due to laser-induced sample heating.[23]

 © 2005 Wiley-VCH Verlag GmbH & Co. KGaA, Weinheim

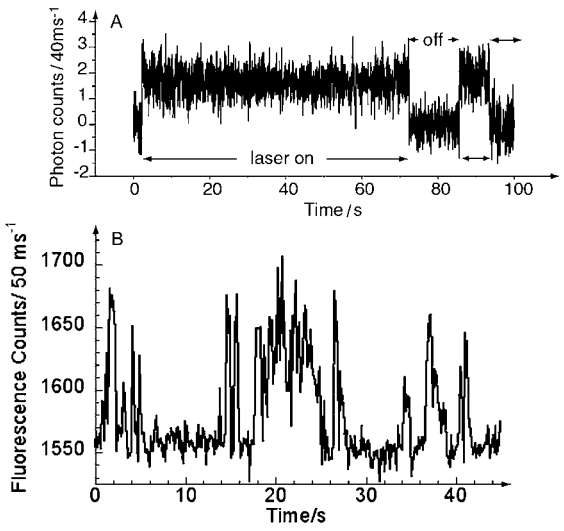

Figure 10. *A) Time trace of a SWNT fluorescence signal in intervals of 40 ms. The excitation was physically blocked during the "off" periods. B) Time trace of a CdSe quantum dot fluorescence signal in intervals of 150 ms.*

The use of single-photon sources is extremely desirable for applications in quantum optics, such as quantum cryptography, since the presence of even two photons in a signal pulse is an opportunity for an eavesdropper to steal or manipulate information.[36] Thus, single molecules or single nanoparticles are attractive as single-photon "on demand" sources in quantum optics. However, their unavoidable fluorescence intermittency drastically hampers their potential utility. For example, in quantum cryptography it is difficult for the receiver to determine whether an "off" period is related to the information being transferred, or just the result of a random blinking event. Some stable sources of single photons do exist, such as nitrogen vacancies in diamond nanoparticles.[37] However, these sources have a very broad linewidth typically over 100 nm, thus limiting the bandwidth of any potential devices.

SWNTs have many advantages for possible use as single-photon sources for quantum optics applications. On the millisecond to minutes time scale, and at room temperature, SWNT fluorescence is stable showing no signs of intensity or spectral blinking. SWNTs also have an extremely narrow linewidth, and can be pumped electrically,[22] which allows for the exciting possibility of future nanometer scale integrated single-photon photonic devices. SWNTs also are resistant to photobleaching, as their fluorescence intensity does not change despite hours of intense photoillumination. Finally, unlike dye molecules or impurities in diamond, SWNTs have an easily size-tunable emission that is in the infrared at technologically relevant wavelengths (1.3–1.5 μm).

Single-molecule sources are also highly desirable for applications in biology and biotechnology. For example, the use of single fluorophores to track individual molecules inside a cell is a compelling method for studying intracellular processes.[38] However, photobleaching of organic dye labels severely restricts the single-molecule processes that can be studied in cells.[38] Detection of a single analyte as reported through changes in the optical emission of a single fluorophore is also a promising approach to achieving the ultimate in detection sensitivity. On the other hand the fluorescence intermittency of single molecules makes the fluorometric detection of single analytes extremely difficult, since the modulation of fluorescence upon binding of the analyte cannot be distinguished from a random blinking event.

SWNTs hold great promise for possible use as single-molecule fluorophores. First, SWNT fluorescence does not photobleach at 300 K even after hours of continuous laser excitation. Thus, extremely long-lived biological processes on the single-molecule level can be followed much more easily. Second, the fact that SWNTs do not exhibit fluorescence blinking allows them to be used as fluorometric reporters of a single biological agent. SWNT photonic devices show strong near-infrared (NIR) electroluminescence,[22] allowing for easy "on-chip" integration of single SWNT sensors with silicon technology. Finally, SWNTs are optically active at wavelengths in the range of 800–1100 nm, which allows for NIR excitation and detection. This NIR optical activity has the tremendous advantage that background fluorescence from the sample can be dramatically reduced allowing for much improved sensitivity on the single fluorophore level.

For some nanoparticles the processes that contribute to fluorescence blinking events slow down as the temperature is lowered. For example, in CdSe semiconductor nanocrystals a higher fraction of nanoparticles are "on" (or bright) at low temperatures versus at room temperature.[30] Interestingly, at low temperatures ($T = 1.8$ K) a significant fraction (about 2/3) of SWNTs show an intermittency in their fluorescence intensity, and also a spectral wandering of their fluorescence energy as shown in Figure 11, and as also was recently reported in ref. [39]. Spectral diffusion cannot be observed at room temperature, since the fluorescence linewidth is much larger than the change in energy during a spectral jump. However, it is currently unclear whether the processes that cause blinking "turn on" at low temperatures, or whether SWNTs blink inherently on timescales much faster than 10 ms. With the time resolution of past experiments, fluctuations in the sub-millisecond regime were not observable.

4. Conclusions

Combined fluorescence and Raman scattering measurements on the single molecule level open up new ways to characterize SWNTs. Single nanotube studies enable the connection between fluorescence energy, (n,m) structural parameters, and RBM frequency of a particular SWNT with a single measurement, and without any complicated fitting procedures[11,16] necessitated by working with macroscopic samples. Single nanotube studies also reveal new insights into nanotube optical properties, such as a variation of the fluorescence energies of nanotubes having the same structure. Unlike for single molecules, for SWNTs the photoluminescence unexpectedly does not show any intensity or spectral fluctuations at room temperature. The fact that SWNTs show no emission intensity blinking or bleaching demonstrates that SWNTs have the po-

 © 2005 Wiley-VCH Verlag GmbH & Co. KGaA, Weinheim

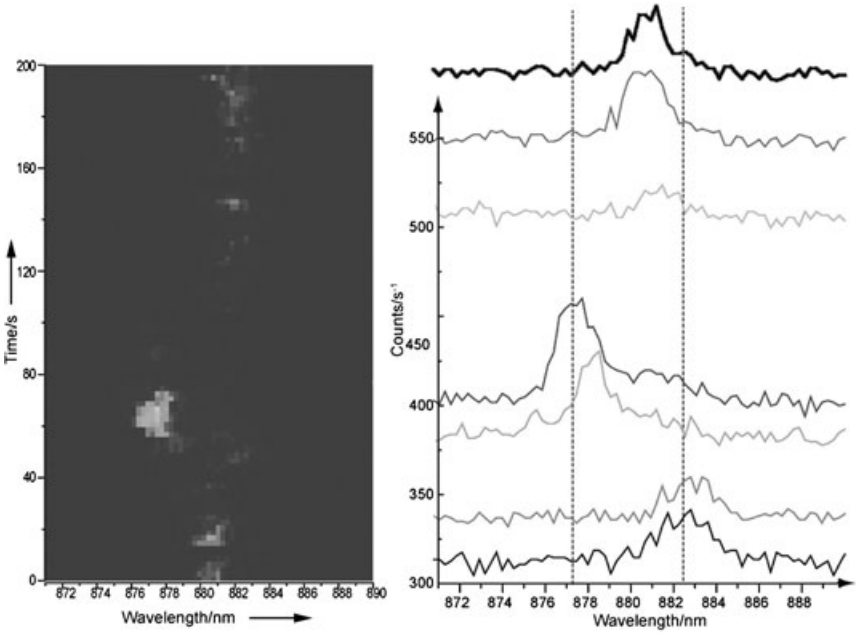

Figure 11. *Temporal evolution of the SWNT fluorescence spectrum at* T = *1.8 K. The right panel represents specific spectra extracted from the left panel, clearly showing evidence of spectral diffusion and intensity blinking.*

tential to provide a stable, single molecule infrared photon source, with an extremely narrow linewidth, which would have a significant impact for future nanometer scale integrated photonic devices and which shows promise for applications in quantum optics and biological sensing.

Acknowledgements

The authors thank Matt Yates for use of equipment. This work was funded by the Department of Energy (DE-FG02-01ER15204), the Air Force Office of Scientific Research (F-49620-03-1-0379), the Research Corporation (grant no. R-10733) and the New York State Office of Science and Academic Research (grant no. C-020085).

Keywords: fluorescence spectroscopy · fluorescence · nanotubes · single-molecule studies

[1] R. Saito, G. Dresselhaus, M. S. Dresselhaus, *Physical Properties of Carbon Nanotubes*, Imperial College Press, London, **1999**.
[2] C. Dekker, *Phys. Today* **1999**, *52*, 22 – 28.
[3] P. G. Collins, P. Avouris, *Sci. Am.* **2000**, *283*, 62 – 69.
[4] C. M. Lieber, *Sci. Am.* **2000**, *285*, 58 – 64.
[5] T. W. Odom, J. L. Huang, P. Kim, C. M. Lieber, *Nature* **1998**, *391*, 62 – 64.
[6] J. W. G. Wildoer, L. C. Venema, A. G. Rinzler, R. E. Smalley, C. Dekker, *Nature* **1998**, *391*, 59 – 62.
[7] M. S. Dresselhaus, G. Dresselhaus, P. C. Eklund, *Science of Fullerenes and Carbon Nanotubes*, Academic Press, San Diego, **1996**.
[8] P. Kim, T. W. Odom, J. L. Huang, C. M. Lieber, *Phys. Rev. Lett.* **1999**, *82*, 1225 – 1228.
[9] S. Reich, C. Thomsen, P. Ordejon, *Phys. Rev. B* **2002**, *65*, 155411 – 1554111.
[10] M. J. O'Connell, S. M. Bachilo, C. B. Huffman, V. C. Moore, M. S. Strano, E. H. Haroz, K. L. Rialon, P. J. Boul, W. H. Noon, C. Kittrell, J. Ma, R. H. Hauge, R. B. Weisman, R. E. Smalley, *Science* **2002**, *297*, 593 – 596.
[11] S. M. Bachilo, M. S. Strano, C. Kittrell, H. Hauge Robert, R. E. Smalley, R. B. Weisman, *Science* **2002**, *298*, 2361 – 2366.
[12] V. C. Moore, M. S. Strano, E. H. Haroz, R. H. Hauge, R. E. Smalley, J. Schmidt, Y. Talmon, *Nano Lett.* **2003**, *3*, 1379 – 1382.
[13] L. Huang, H. N. Pedrosa, T. D. Krauss, *Phys. Rev. Lett.* **2004**, *93*, 0174031 – 0174034.
[14] H. Kataura, Y. Kumazawa, Y. Maniwa, I. Umezu, S. Suzuki, Y. Ohtsuka, Y. Achiba, *Synth. Met.* **1999**, *103*, 2555 – 2558.
[15] R. Saito, G. Dresselhaus, M. S. Dresselhaus, *Phys. Rev. B* **2000**, *61*, 2981 – 2990.
[16] A. Hagen, T. Hertel, *Nano Lett.* **2003**, *3*, 383 – 388.
[17] C. L. Kane, E. J. Mele, *Phys. Rev. Lett.* **2003**, *90*, 2074011 – 2074014.
[18] C. D. Spataru, S. Ismail-Beigi, L. X. Benedict, S. G. Louie, *Phys. Rev. Lett.* **2004**, *92*, 0774021 – 0774024.
[19] S. Lebedkin, F. Hennrich, T. Skipa, M. M. Kappes, *J. Phys. Chem. B* **2003**, *107*, 1949 – 1956.
[20] J. Lefebvre, Y. Homma, P. Finnie, *Phys. Rev. Lett.* **2003**, *90*, 2174011 – 2174014.
[21] S. M. Bachilo, L. Balzano, J. E. Herrera, F. Pompeo, D. E. Resasco, R. B. Weisman, *J. Am. Chem. Soc.* **2003**, *125*, 11186 – 11187.
[22] J. A. Misewich, R. Martel, P. Avouris, J. C. Tsang, S. Heinze, J. Tersoff, *Science* **2003**, *300*, 783 – 786.
[23] A. Hartschuh, H. N. Pedrosa, L. Novotny, T. D. Krauss, *Science* **2003**, *301*, 1354 – 1356.
[24] T. W. Tombler, C. W. Zhou, L. Alexseyev, J. Kong, H. J. Dai, L. Lei, C. S. Jayanthi, M. J. Tang, S. Y. Wu, *Nature* **2000**, *405*, 769 – 772.
[25] H. W. C. Postma, T. Teepen, Z. Yao, M. Grifoni, C. Dekker, *Nature* **2001**, *293*, 76 – 79.
[26] M. Bockrath, W. J. Liang, D. Bozovic, J. H. Hafner, C. M. Lieber, M. Tinkham, H. K. Park, *Science* **2001**, *291*, 283 – 285.
[27] M. T. Woodside, P. L. McEuen, *Science* **2002**, *296*, 1098 – 1101.
[28] P. L. McEuen, M. Bockrath, D. H. Cobden, Y. G. Yoon, S. G. Louie, *Phys. Rev. Lett.* **1999**, *83*, 5098 – 5101.
[29] M. Nirmal, B. O. Dabbousi, M. G. Bawendi, J. J. Macklin, J. K. Trautman, T. D. Harris, L. E. Brus, *Nature* **1996**, *383*, 802 – 804.
[30] K. T. Shimizu, R. G. Neuhauser, C. A. Leatherdale, S. A. Empedocles, W. K. Woo, M. G. Bawendi, *Phys. Rev. B* **2001**, *63*, 2053161 – 2053165.
[31] M. Kuno, D. P. Fromm, H. F. Hamann, A. Gallagher, D. J. Nesbitt, *J. of Chem. Phys.* **2000**, *112*, 3117 – 3120.
[32] S. Empedocles, M. Bawendi, *Acc. Chem. Res.* **1999**, *32*, 389 – 396.
[33] J. K. Trautman, J. J. Macklin, L. E. Brus, E. Betzig, *Nature* **1994**, *369*, 40 – 42.
[34] R. M. Dickson, A. B. Cubitt, R. Y. Tsien, W. E. Moerner, *Nature* **1997**, *388*, 355 – 358.
[35] W. E. Moerner, M. Orrit, *Science* **1999**, *283*, 1670 – 1676.
[36] B. Lounis, W. E. Moerner, *Nature* **2000**, *407*, 491 – 493.
[37] A. Beveratos, R. Brouri, T. Gacoin, A. Villing, J.-P. Poizat, P. Grangier, *Phys. Rev. Lett.* **2002**, *89*, 1879011 – 1879014.
[38] M. Dahan, S. Levi, C. Luccardini, P. Rostaing, B. Riveau, A. Triller, *Science* **2003**, *302*, 442 – 445.
[39] H. Htoon, M. J. O'Connell, P. J. Cox, S. K. Doorn, V. I. Klimov, *Phys. Rev. Lett.* **2004**, *93*, 0274011 – 0274014.

Received: August 27, 2004
Published online on ■■ ■■, 2005

 © 2005 Wiley-VCH Verlag GmbH & Co. KGaA, Weinheim